Organic Electronics 10 (2009) 115–118

Contents lists available at ScienceDirect

Organic Electronics

journal homepage: www.elsevier.com/locate/orgel

Negative capacitance and its photo-inhibition in organic bulk heterojunction devices

C. Lungenschmied [a,1], E. Ehrenfreund [a,b,*], N.S. Sariciftci [a]

[a] Linz Institute for Organic Solar Cells (LIOS), Johannes Kepler University, 4040 Linz, Austria
[b] Physics Department, Technion, Israel Institute of Technology, Haifa 32000, Israel

ARTICLE INFO

Article history:
Received 21 April 2008
Received in revised form 8 September 2008
Accepted 9 October 2008
Available online 1 November 2008

PACS:
73.50.Gr
73.50.Pz
73.61.Ph
73.61.Wp

Keywords:
Negative capacitance
P3HT:PCBM heterojunctions
Solar cells
Photo-capacitance

ABSTRACT

We report the dynamic admittance, both in the dark and under illumination, of heterojunctions made of poly(3-hexyl thiophene)/1-(3-methoxycarbonyl)propyl-1-phenyl[6,6]C_{61} (P3HT:PCBM) blends, which are used in efficient organic solar cells. In the dark there appears a huge low frequency negative capacitance which we associate with slow electron hole bimolecular recombination at the heterojunction interfaces. Surprisingly, under photoexcitation the negative capacitance gradually disappears with increasing light intensity. We attribute this positive photoinduced capacitance to the combined effect of (1) long lived photogenerated charges at the P3HT:PCBM interfaces that increase electron-hole bimolecular recombination rate, which in turn renders the capacitance less negative and (2) trapped photogenerated charges that increase the capacitance upon re-emission.

1. Introduction

We report a huge dark negative capacitance (NC) and its disappearance under illumination in organic bulk heterojunction devices made of poly(3-hexylthiophene)(P3HT) and 1-(3-methoxy carbonyl)propyl-1-phenyl[6,6]C_{61} (PCBM). Photovoltaic cells based on P3HT:PCBM blends are among the most efficient in this class of devices [1–4]. The NC phenomenon in various devices, such as inorganic Schottky diodes, inorganic homojunction photodetectors, organic light emitting devices and more, has been reported previously, while its origin is still under debate [5–9]. In many cases, the frequency, ω, dependence of the NC spectrum, $C(\omega)$, has been shown to be directly related to current relaxation [5,6] or electron–hole (e–h) recombination in bipolar organic devices [7,9]. The primary cause for the NC is probably different in different systems. In the present case of organic heterojunction devices, the NC is observed under bipolar charge injection conditions. At low enough frequencies the NC saturates reaching (in absolute value) up to ≈500 times the geometrical capacitance at low frequencies. The bias voltage and frequency dependencies of NC enable us to determine the e–h bimolecular recombination (BMR), which is responsible for the spectral behavior of the NC and the corresponding dynamic sample conductance.

Upon photoexcitation the NC diminishes in magnitude and the capacitance reaches even positive values under sufficiently intense illumination. We attribute this positive photoinduced capacitance to the combined effect of (1)

* Corresponding author. Address: Physics Department, Technion, Israel Institute of Technology, Haifa 32000, Israel. Tel.: +972 4829 3610; fax: +972 4823 5107.
E-mail address: eitane@tx.technion.ac.il (E. Ehrenfreund).
[1] Present address: Konarka Austria GmbH, Altenbergerstrasse 69, 4040 Linz, Austria.

1566-1199/$ - see front matter © 2008 Elsevier B.V. All rights reserved.
doi:10.1016/j.orgel.2008.10.011

long lived photogenerated charges at the P3HT:PCBM interfaces that increase e–h BMR rate, which in turn renders the capacitance less negative and (2) trapped photogenerated charges that increase the capacitance upon re-emission.

2. Experimental

Thoroughly cleaned indium tin oxide (ITO) covered glass slides are used as substrate. An $L \approx 800$ nm thick photo-active layer made from a regio-regular (rr)-P3HT:PCBM solution (1:1, 2% in chloroform) was cast by the doctor blade technique on the substrate. The Al top contacts were applied by vacuum deposition, followed by an annealing step (5 min at 120 °C). The diodes (active area $A \simeq 12$ mm^2) showed a rectification ratio of $\simeq 10^4$ at ±1 V (Fig. 4, inset). Forward (positive) bias conditions are obtained when the ITO is wired (+) and Al wired (−). An HP 4284A LCR-meter operated in the frequency range $f = \omega/2\pi = 20 - 10^6$ Hz (20 mV ac voltage) was used to measure the complex admittance $Y(\omega)$, from which the capacitance $C(\omega) = ImY(\omega)/\omega$ and the conductance $G(\omega) = ReY(\omega)$ were extracted. We carefully analyzed the low frequency regime in order to make sure that the extracted $C(\omega)$ and $G(\omega)$ are not influenced by any parasitic circuit reactance [10]. The 532 nm line of a Nd:YVO_4 laser was used as light source for the photoinduced admittance measurements. All measurements reported here were done at room temperature.

3. Results

In Fig. 1 we display the measured frequency dependent capacitance of the ITO-P3HT:PCBM-Al device in the dark at various applied forward bias voltages. For $V_{bias} > 0.3$ V, we observe a negative contribution to the capacitance and relate it to current relaxation [5] due to e–h recombination in the bipolar injection regime [6,9]. This negative contribution becomes more dominant as the voltage increases above 0.35 V, where $C(\omega)$ becomes more negative as the bias increases. The effect of increasing bias on NC is shown in the inset of Fig. 1 where the measured capacitance at 50 Hz, $C(50\text{ Hz})$, is plotted as a function of V_{bias}. At 1.5 V, $C(50\text{ Hz}) \approx -200$ nF, which is (in absolute value) $\simeq$500 times the geometrical capacitance, $C_g = \varepsilon A/L \simeq 0.4$ nF ($\varepsilon \simeq 3\varepsilon_0$ is the sample static dielectric constant and ε_0 is the vacuum permittivity).

The decrease in capacitance as f decreases below ≈5–10 kHz, is accompanied by a corresponding increase in the conductance, as shown in the inset to Fig. 2. The zero value $G(f \approx 0)$ corresponds to the static conductance dI/dV. Denoting $\Delta G(f) \equiv G(0) - G(f)$, the quantity $\Delta G(f)/f$ (up to $f \approx 10$ kHz) is proportional [11] to the corresponding changes in $\varepsilon''(f)$, the imaginary part of the dielectric function associated with the process. In Fig. 2, $\Delta G(f)/f$ is displayed for various bias voltages, showing the bell shaped curves characteristic to ε''. Note the shift of the curves' maximum towards higher frequencies for higher bias; this is consistent with the observed faster recombination process at higher voltages (see discussion below).

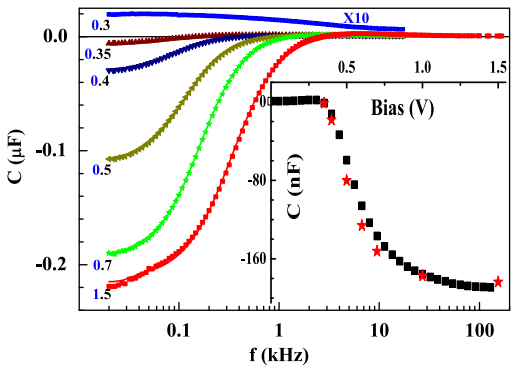

Fig. 1. Frequency dependent capacitance measured on an ITO-P3HT:PCBM-Al device shown for various forward bias from 0.3 to 1.5 V (as marked). Symbols: data points, solid lines: fits to the data. The 0.3 V data is multiplied by 10 for clarity. Inset: $C(50\text{ Hz})$ vs bias voltage. Black squares – data points and red stars – fit (see text).

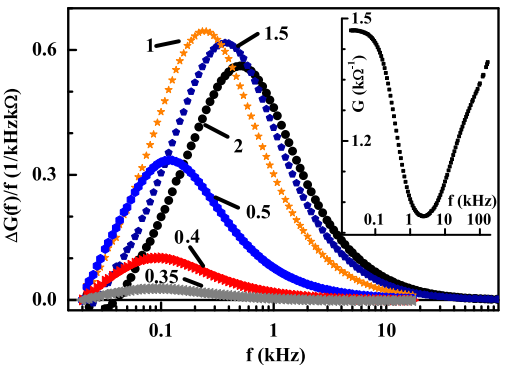

Fig. 2. The frequency dependence of $\Delta G(f)/f \equiv [G(20\text{ Hz}) - G(f)]/f$ for the same device as in Fig. 1, showing the typical bell shaped loss function behavior. Symbols: data points at various bias voltages (in V) as marked. Inset: $G(f)$ vs f for $V_{bias} = 1.5$ V.

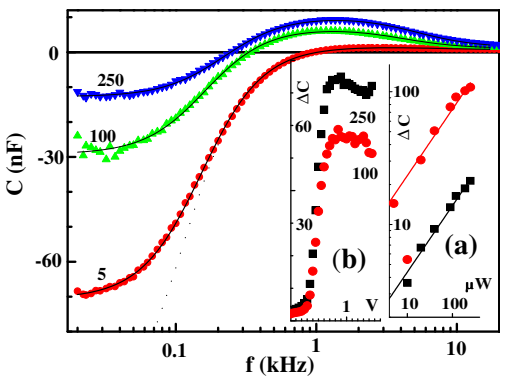

Fig. 3. The capacitance of the ITO-P3HT:PCBM-Al device vs frequency measured under laser illumination (532 nm) at $I_L = 5$, 100, 250 μW, as marked ($V_{bias} \simeq 0.6$ V). For clarity, only the frequency range 0.02–15 kHz is shown. Inset (a): the photoinduced changes $\Delta C \equiv C_{light} - C_{dark}$ (in nF) at $f = 50$ Hz vs I_L (on a log–log plot) for $V_{bias} = 0.35$ (black square) and 0.5 V (red dots) The solid lines are fits to $\Delta C \propto I_L^{1/2}$ law. Inset (b): ΔC (in nF) at $f = 50$ Hz vs V_{bias} for $I_L = 100$ μW (red dots) and 250 μW (black square).

We now turn to the effect of photoexcitation on NC. In Fig. 3 the measured capacitances of a ITO-P3HT:PCBM-Al device under 532 nm continuous irradiation (C_{light}) are shown in the bipolar charge injection regime for various light intensities, I_L. A significant increase in the capacitance due to illumination is observed at low frequencies. Above 15 kHz up to 1 MHz the photoinduced changes in the capacitance are very small (not shown in Fig. 3). The photoinduced changes in the capacitance, $\Delta C \equiv C_{light} - C_{dark}$, are sensitive to both the light intensity and applied bias. Inset (a) to Fig. 3 shows the dependence of $\Delta C(50\,Hz)$ on I_L at fixed V_{bias}. The observed $\Delta C \propto I_L^{1/2}$ for both $V_{bias} = 0.35$ and 0.5 V is indicative of a BMR mechanism for the photoinduced carriers. Inset (b) to Fig. 3 shows the dependence of $\Delta C(50\,Hz)$ on V_{bias} at fixed I_L. Below $V_{bias} \approx 0.35$ V $\Delta C(50\,Hz) \leqslant$ 3–4 nF, then a sharp rise at $V_{bias} \approx 0.35$ V followed by a plateau (where $\Delta C(50\,Hz) \geqslant$ 100 nF for $I_L \geqslant 100\ \mu W/cm^2$) above ≈0.6 V are evident.

4. Discussion

The negative contribution to the dark $C(\omega)$ is observed here only at $V_{bias} > 0.3$ V, under the conditions of bipolar injection. NC is more pronounced at higher forward bias voltages, where the conductance of the device is higher. The maximum frequency at which NC is observed is restricted approximately to $f < 2$ kHz at $V_{bias} = 1.5$ V where NC is most pronounced. Such low frequencies represent time scales which are much longer than the single carrier transit time in this device (≃5 μs at 1 V). It is therefore plausible to analyze the NC as a separate process dominating the other transport processes in this frequency range. Previously, such an approach was used by Penin [5] in order to account for NC in semiconductor Schottky diodes via impact ionization of impurity atoms and in GaAs homojunctions via interface states mediated recombination [6]. In our previous publication [9] we have shown that the NC spectrum measured in organic semiconductor devices could be accurately described when treating NC as a separate mechanism in addition to the effect of space charge. In all these approaches the recombination plays an important role. Under bipolar injection conditions (with dc conductance $G_0 = dI/dV$) and for a finite recombination time, τ_r, a negative contribution (of the order of $\tau_r G_0$) to the capacitance should be expected at frequencies $\omega < \tau_r^{-1}$; this is similar to the negative contribution to the capacitance which occurs simultaneously with an increase in conductance at frequencies below the reciprocal transit time in a unipolar SCLC device. The effect of recombination on the capacitance and conductance can be summarized as follows [5,6,9]:

$$C_r(\omega) = -\frac{G_{r0}\tau_r}{1+\omega^2\tau_r^2}; \quad G_r(\omega) = G_{r0} - \frac{G_{r0}\omega^2\tau_r^2}{1+\omega^2\tau_r^2}, \qquad (1)$$

where G_{r0} is the conductance associated with the process. As can be seen from Eq. (1), the maximum of the conductance (and most negative capacitance) occurs for $\omega \ll \tau_r^{-1}$ near $\omega \approx 0$; at higher frequencies the conductance decreases due to the diminishing carrier density ($\propto (\omega\tau_r)^{-2}$ for $\omega \gg \tau_r^{-1}$) and the capacitance becomes less negative. It is important to note that the shorter is the recombination time, the wider is the frequency range in which NC can be observed experimentally. We can now use Eq. (1) in order to fit the data in the bipolar injection regime ($V_{bias} \geqslant 0.35$ V in Fig. 1). In the relevant range where the NC is dominant (up to 5 kHz), the fits (solid lines, Fig. 1) account very well for $C(\omega)$. In particular, we notice the experimentally observed leveling off of $C(f)$ below 30–40 Hz, that is very well accounted for by Eq. (1). Furthermore, the voltage dependence of C is also fully explained by our analysis, as can be seen in the inset to Fig. 1, where the stars denote the capacitance calculated using the parameters obtained from the frequency fits at each voltage.

The losses due to e–h recombination in the bipolar injection regime are clearly revealed in the $\Delta G(f)/f$ plots shown in Fig. 2. The changes $\Delta\varepsilon''(\omega) \equiv [G_r(0) - G_r(\omega)]/\omega = G_{r0}\omega\tau_r^2/(1+\omega^2\tau_r^2)$ (Eq. (1)), can be ascribed to the losses due to recombination. As formally expected from the inter-relation between $C(f)$ and $G(f)$, exactly the same parameters, τ_r and G_{r0}, obtained from the $C(\omega)$ fits in Fig. 1, account accurately for the peak frequency and peak height of $\Delta G(f)/f$ in Fig. 2.

Interestingly, the voltage dependence of the fitted conductance, G_{r0}, follows exactly that of the static conductance, dI/dV, as seen in Fig. 4, where we find that $G_{r0}(V) \propto dI/dV$ for the entire bias range. The proportionality of the fitted G_{r0} (from the complex admittance experiment, Figs. 1 and 2) and the measured dI/dV (from the dc I–V experiment, Fig. 4, inset) further supports the interconsistency of the experimental results.

The recombination rate, τ_r^{-1}, extracted from the fits shows a linear dependence on V_{bias}, as shown in Fig. 4. From the dI/dV curve we see that bipolar injection (as well as NC) starts at $V_{bias} \simeq 0.35$ V; thus the actual injection voltage is $V = V_{bias} - 0.35$ V. The straight dashed line in Fig. 4 is a linear fit to the data. The linear dependence on V implies a BMR mechanism under bipolar injection, where the average BMR rate, τ_{BM}^{-1}, may then be written as [12]

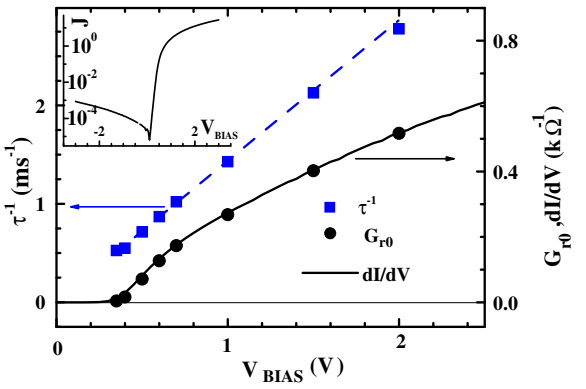

Fig. 4. The recombination parameters τ_r^{-1} (left axis) and G_{r0} (right axis), extracted from the fits to the NC data of Fig. 1, are shown vs V_{bias}. The straight dashed line is a linear fit, $1/\tau_r(m\,s^{-1}) = 0.55 + 1.45(V_{bias} - 0.35\ V)$. The static admittance dI/dV (multiplied by 0.3) is overlayed (right axis) on the extracted G_{r0} for comparison. Inset: current density J (in mA/cm^2) vs V_{bias} (in V).

$$\tau_{BM}^{-1} = \gamma\bar{n} = \frac{4V}{L^2}\left[\frac{\mu_n\mu_p\varepsilon\gamma}{2e(\mu_n+\mu_p)}\right]^{1/2}, \quad (2)$$

where $\gamma = \bar{v}\sigma_R$ is the BMR coefficient, $\bar{v}$ is the average e–h microscopic relative velocity, σ_R is their recombination cross section, and $\bar{n}$ is the average carrier density. The measured mobility of the carriers in annealed rrP3HT:PCBM is of the order $\mu \approx 10^{-3}$ cm^2/Vs for both electrons and holes [13]. The linear fit of the data in Fig. 4 then yields $\gamma \simeq 10^{-12}$ cm^3/s, similar to the value observed by other techniques [7,14,15]. This BMR coefficient, γ, is $\simeq 10^3$ times smaller than the Langevin BMR coefficient: $\gamma_L = 2e(\mu_n+\mu_p)/\varepsilon$. Obviously, a high recombination coefficient inhibits the efficiency of organic photovoltaic devices. The reduced BMR coefficient has been suggested to be the result of different pathways for electrons and holes in the heterojunction device [14,16]. Being confined to different phases or pathways, electrons and holes would recombine only at the interfaces between the phases. Thus the volume in which the recombination occurs is only a small fraction of the total volume in which the current flows.

Under bipolar injection, where the NC is dominant, it is surprising that by adding photoinduced carriers the NC decreases in magnitude, as shown in Fig. 3. Moreover, the reduction in NC, ΔC, increases dramatically in forward bias as seen in Fig. 3 (inset (b)). Inset (a) of Fig. 3 shows that $\Delta C \propto I_L^{1/2}$. Assuming that ΔC is proportional to the steady state density of the photogenerated carriers, the square root dependence on I_L implies that the photogenerated carriers undergo BMR process, in agreement with previous observations [14].

The photoinduced positive contribution ΔC increases sharply at the onset of bipolar injection. It may therefore be related to the phenomenon of negative capacitance, which also appears only under bipolar injection. Such inhibition of the negative capacitance may be due to an increase in recombination rate by the photoinduced carriers decreasing thereby the magnitude of the NC, according to Eq. (1). Such photo-enhancement of the BMR may not be surprising since the photoinduced charges are predominantly created at the heterojunctions, where the local electric field breaks the photoexcited excitons. The increased carrier density at the heterojunction, where most of the bimolecular recombination takes place, shortens thus the recombination time. Alternatively, positive ΔC may arise from trapped photoinduced carriers: upon re-emission from the traps the capacitance increases [17]. The effect of traps may be more evident from the maximum observed in the spectrum of $C_{light}(f)$ at around $f \simeq 1$ kHz (Fig. 3 at I_L = 100 and 250 μW). It is plausible that the 532 nm illumination excites deep compensated donors or acceptors, which may then become deep traps for the injected carriers. If the emission rate from these photogenerated traps (PGT) is e_{PGT}, then the increase of the capacitance due to the traps is $\Delta C_{PGT}(\omega) \propto 1/(1+\omega^2/e_{PGT}^2)$ [18]. Taking now into consideration both the effect of NC inhibition (i.e. reduced NC under light) and the PGT contribution (ΔC_{PGT}), the frequency dependent admittance data under illumination at I_L = 0.1 and 0.25 μW is very well accounted for with $e_{PGT} \simeq 3\times10^4$ s^{-1} (Fig. 3, solid lines). Emission rates of the same order of magnitude were previously found for deep traps in organic diodes [19].

5. Summary

In summary, we have shown that in bulk heterojunction diodes made of annealed composites of rrP3HT and PCBM and under forward bias conditions a huge (up to $\simeq 500 C_g$) negative capacitance is observed. We show that finite electron hole recombination times make it possible to observe the negative capacitance in the bipolar injection regime. We extract the bimolecular recombination coefficient and show that it is ≈1000 smaller than the Langevin value. Under illumination, the total capacitance becomes less negative reaching even positive values at sufficient intensities. This phenomenon may arise from an enhancement of the BMR rate at the heterojunction interfaces due to the extra carrier photoinduced density at exactly these donor–acceptor interfaces. Alternatively, it may arise from trapped photoinduced carriers.

Acknowledgements

We thank Dr. G. Dennler for very valuable discussions. This work has been supported by the Austrian fund for the Advancement of Science (FWF, S9711-NO8). E.E. acknowledges the support of the Israel Science Foundation (ISF 745/08).

References

[1] P. Schilinsky, C. Waldauf, C.J. Brabec, Appl. Phys. Lett. 81 (2002) 3885.
[2] F. Padinger, R. Rittberger, N.S. Sariciftci, Adv. Funct. Mater. 13 (2003) 85.
[3] Y. Kim, S.A. Choulis, J. Nelson, D.D.C. Bradley, S. Cook, J.R. Durrant, Appl. Phys. Lett. 86 (2005) 063502.
[4] W. Ma, C. Yang, X. Gong, K. Lee, A.J. Heeger, Adv. Funct. Mater. 15 (2005) 1617.
[5] N.A. Penin, Semiconductors 30 (1996) 340.
[6] A.G.U. Perera, W.Z. Shen, M. Ershov, H.C. Liu, M. Buchanan, W.J. Schaff, Appl. Phys. Lett. 74 (1999) 3167.
[7] H.H.P. Gommans, M. Kemerink, R.A.J. Janssen, Phys. Rev. B 72 (2005) 235204.
[8] N.D. Nguyen, M. Schmeits, H.P. Loebl, Phys. Rev. B 75 (2007) 075307.
[9] E. Ehrenfreund, C. Lungenschmied, G. Dennler, H. Neugebauer, N.S. Sariciftci, Appl. Phys. Lett. 91 (2007) 012112.
[10] K.S.A. Butcher, T.L. Tansley, D. Alexiev, Solid State Electron. 39 (1996) 333.
[11] K.L. Ngai, R.W. Rendell, Dielectric and conductivity relaxation in conducting polymers, in: T.A. Skotheim (Ed.), Handbook of Conducting Polymers, vol. 2, 1986 (Chapter 28).
[12] M.A. Lampert, P. Mark, Current Injection in Solids, Academic Press, New York, 1970.
[13] A. Pivrikas, N.S. Sariciftci, G. Juška, R. Österbacka, Prog. Photovolt: Res. Appl. 15 (2007) 677.
[14] A. Pivrikas, G. Juška, A.J. Mozer, M. Scharber, K. Arlauskas, N.S. Sariciftci, H. Stubb, R. Österbacka, Phys. Rev. Lett. 94 (2005) 176806.
[15] G. Juška, G. Sliauzys, K. Genevičius, K. Arlauskas, A. Pivrikas, M. Scharber, G. Dennler, N.S. Sariciftci, R. Österbacka, Phys. Rev. B 74 (2006) 115314.
[16] L.J.A. Koster, V.D. Mihailetchi, P.W.M. Blom, Appl. Phys. Lett. 88 (2006) 052104.
[17] H.C.F. Martens, H.B. Brom, P.W.M. Blom, Phys. Rev. B 60 (1999) 8489.
[18] G. Vincent, D. Bois, P. Pinard, J. Appl. Phys. 46 (1975) 5173.
[19] O. Gaudin, R.B. Jackman, T.-P. Nguyen, P.L. Rendu, Mat. Res. Soc. Symp. Proc. 725 (2002) P11.7.